Desalination and Water Treatment
www.deswater.com

doi:10.5004/dwt.2017.11080

61 (2017) 306–310
January

Numerical simulation of horizontal-tube falling film evaporation using VOF method

Luopeng Yang*, Yan Yang, Hongyou Li, Yang Liu, Shengqiang Shen

Key Laboratory of Ocean Energy Utilization and Energy Conservation of Ministry of Education, Dalian University of Technology, Dalian, 116024, China, Tel. +86-411-84708460; Fax +86-411-84707963; email: yanglp@dlut.edu.cn

Received 14 April 2015; Accepted 18 October 2016

ABSTRACT

Hydrodynamics and heat transfer of falling film evaporation on a horizontal tube was numerically investigated using the volume of fluid (VOF) method which is suitable to track the dynamic interface between phases of vapor and liquid. Profiles of local temperatures, velocity, film thickness and heat transfer coefficient within liquid film were calculated. The predictions agreed well with the experimental data. The results show that the variation of viscosity, surface tension, and thermal conductivity in liquid film, caused by the temperature distribution, has an obvious effect on heat transfer coefficients even at low Reynolds numbers. An increase in local heat transfer coefficient and a decrease in local film thickness along the tube circumference are observed in the thermal developing region due to the effects of gravity and decreasing thermal conductivity. Local heat transfer coefficients stabilize at the bottom of the tube where the film is in the thermal developed region.

Keywords: Falling film evaporation; Volume of fluid; Heat transfer coefficient; Film thickness

1. Introduction

Falling film evaporators are widely employed in petro-chemical, refrigeration, power generation and desalination industries due to their principal advantages of high heat transfer rates at small temperature difference and thin liquid film. As the falling film evaporators contain hundreds or thousands of tubes with several meters long, their heat transfer performance results from the complex interaction between the dynamics of both vapor and liquid phases and heat transfer processes determined by the two-phase flow structure. Therefore, the complicated heat and mass transfer phenomena, occurring in the falling film evaporator, have been the subject of a great number of research.

A great deal of experimental and theoretical works on heat transfer and hydrodynamics in falling film evaporation have been performed. The published investigations have focused on experimentally obtaining flow patterns of liquid film which have a significant effect on hydrodynamic and heat transfer of falling film. Attempts were conducted to characterize the flow patterns by visual observations [1–5,12]. The comparison of the proposed flow patterns does not agree well with each other due to the fact that the flow pattern identification depends on the researchers' arbitrary observation. The appearance of dry patches, which has a negative effect on the heat transfer performance and flow stability, has received much attention. Experiments [6–8] were conducted to determine the threshold heat fluxes and Reynolds numbers for film breakdown.

An experimental determination of heat transfer coefficient correlations on a plain tube was obtained as a function of heat flux, saturation temperature, flow rates, nozzle height and nozzle type [9–11]. Most of the experiments were on how the experimental parameters affected heat transfer rates. Little experimental research concerning local hydrodynamics and heat transfer have been performed due to the inherent challenge in measuring local parameters in liquid

*Corresponding author.

Presented at EuroMed 2015: Desalination for Clean Water and Energy Palermo, Italy, 10–14 May 2015. Organized by the European Desalination Society.

film although the local conditions give a real insight to the true nature of liquid and vapor flow and their interactions.

A significant amount of efforts have been developed to mathematically simulate the heat and mass transfer phenomena occurring in falling film evaporation [13–22]. The assumed linear temperature profile was proved to rarely work by the experimental observation [13]. The velocity profiles were assumed to be linear in the thermal boundary developing layer [14], parabolic for laminar films of both the adiabatic and isothermal wall cases [15,16]. The arbitrary assumptions included in their models significantly affect the predicted heat transfer performance since the profiles of temperatures and velocities are determined by fluid motion in liquid film and the interaction between liquid film and vapor.

The objective of the present study is to explore the characteristics of hydrodynamic and heat transfer, which were simulated by a fluent code based on the volume of fluid (VOF) method. The profiles of local temperature, velocity, heat transfer coefficient, and film thickness within liquid film around a tube were predicted. The local information within liquid film contributes to understanding the flowing and energy transportation in the two-phase falling film flow.

2. Numerical model formulation

2.1. Physical model

A schematic of a physical model of horizontal-tube falling film evaporation is presented in Fig. 1. Liquid with an uniform inlet temperature and a mass flow density of Γ impinges on the top of the tube at a height of H = 5 mm. Liquid film flows along the perimeter of the tube and drains down to the bottom of the tube under the combined effect of the gravity, viscous force and surface tension. The liquid film is heated by a tube wall which remains constant temperature or heat flux.

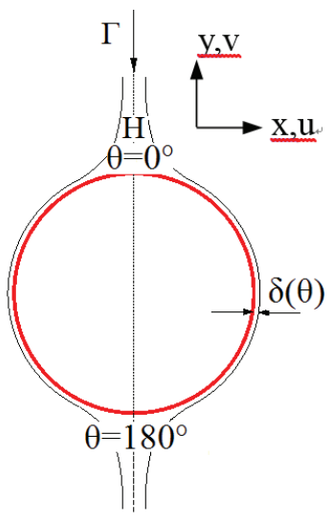

Fig. 1. Schematic of horizontal-tube falling film evaporation.

2.2. Basic assumption

The major assumptions in this model are as follows:

(1) A laminar flow model is used for the falling film in a wavy laminar flow or a transition from laminar to slightly turbulent flow due to the fact that an existing laminar sub-layer dominates the heat transfer resistance within the liquid film.
(2) Thermo-physical properties of the liquid film are functions of temperature.
(3) Vapor pressure surrounding the horizontal tube is set to be constant and corresponds to vapor saturated temperature.
(4) The curvature effect is neglected as the film is thin enough compared with the tube radius.

2.3. Control equations and volume of fraction (VOF) method

The continuity, momentum and energy equations are as follows:

$$\frac{\partial \rho}{\partial t} + \nabla \cdot (\rho \vec{v}) = S_m \tag{1}$$

$$\frac{\partial}{\partial t}(\rho \vec{v}) + \nabla \cdot (\rho \vec{v}\vec{v}) = -\nabla p + \nabla \cdot (\vec{\tau}) + \rho \vec{g} + \vec{F} \tag{2}$$

$$\frac{\partial}{\partial t}(\rho T) + \nabla \cdot (\rho \vec{v} T) = \nabla \cdot \left(\frac{k}{\rho c_p} \nabla T \right) + S_e \tag{3}$$

A VOF model was used to simulate horizontal-tube falling film evaporation. A dynamic liquid–vapor interface of falling film outside a horizontal tube can be tracked by simulating vapor volume fraction in meshes of liquid film at the interface. In the VOF model, user defined function profiles were source functions for liquid film thermo-physical properties and mass transfer rates of evaporation [25]. The fluid thermo-physical properties were calculated by the volume fraction in each cell.

2.4. Mesh generation and boundary conditions

The governing equations combined with the boundary conditions were numerically solved by the fluent code based on the finite volume method. Due to the axial symmetry of falling film around a horizontal tube, half of the falling film was modeled with VOF method. A quadrilateral mesh was utilized and the boundary layer meshes in the adjacent region around the tube wall were refined in Fig. 2. The top boundary of the computational region, where liquid falls downwards uniformly was set as velocity inlet and pressure inlet. The right side and bottom were pressure inlet and pressure outlets, respectively. The left side boundary was set as the symmetry plane.

2.5. Grid independency analysis

A comparison of local film thicknesses for several grid sizes was presented in Fig. 3. A grid independency analysis showed that the accuracy of the film thickness was not

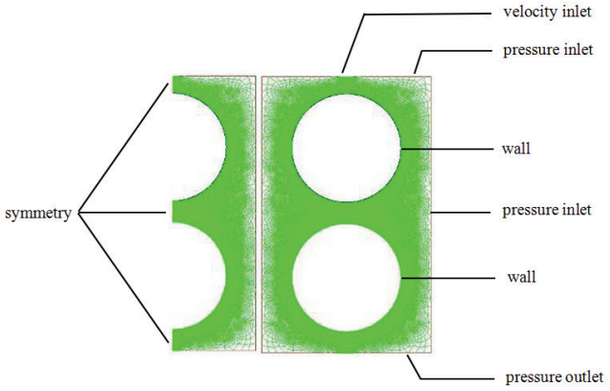

Fig. 2. Schematic of CFD model with boundary conditions.

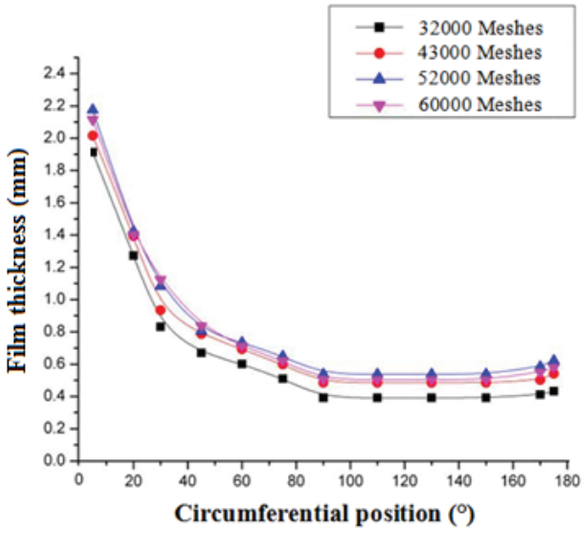

Fig. 3. Grid independence analysis for Γ = 0.18 kg/m·s.

improved considerably beyond 43,000 meshes. Therefore, a grid scheme with 43,000 meshes was chosen for the subsequent simulation cases.

3. Results and discussion

The numerical predictions of non-dimensional heat transfer coefficients, $h^+ = h\left[\mu^2/\left(g\rho^2k^3\right)\right]^{1/3}$, for saturated falling film flowing over a heated horizontal tube with a constant heat flux were compared with experimental results [23] and predictions of Nusselt's correlations in Fig. 4. It is predicted that the simulated results are higher than the solution of Nusselt's condensation. This is due to the fact that the convective term in the energy equation, which is neglected in the Nusselt's solution, is taken into account in the simulation model. The difference between the numerical results and the Struve's experimental data is within 7%. The good agreement verifies that the simulation model is accurate and reliable.

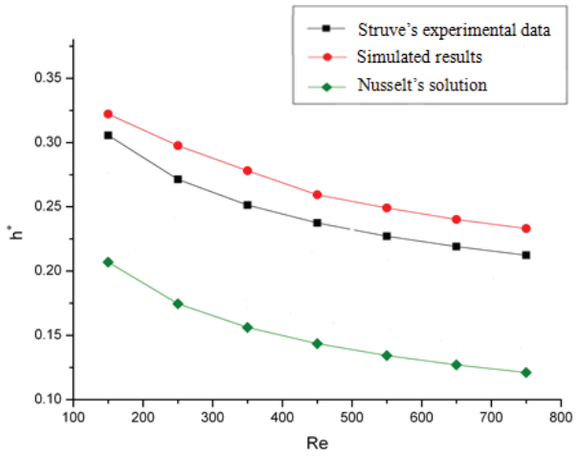

Fig. 4. Comparison of non-dimensional heat transfer coefficients.

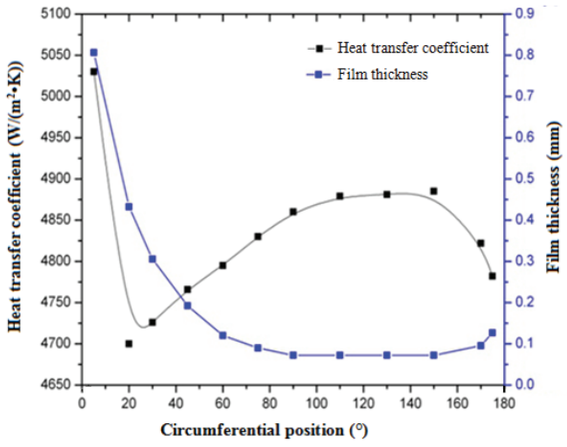

Fig. 5. Profiles of local heat transfer coefficients and film thickness for Re = 450: (a) 0.162 s, (b) 0.279 s, (c) 0.384 s.

Fig. 5 presents the profiles of local heat transfer coefficients and film thicknesses along the tube circumference for Re = 450 with heat transfer temperature difference of ΔT = 2.8°C, saturated evaporation temperature of T_{sat} = 62°C, and tube diameter of 25.4 mm. Local heat transfer coefficient and film thickness at the apex are the highest due to the impinging effect of liquid film and subsequently reduce sharply. In the following thermally developing region where liquid film is heated to its saturated temperature, a decrease in liquid viscosity with increasing film temperature, together with the effect of gravity acceleration, results in a decrease in film thickness and an increase in local heat transfer coefficient. For the thermally developed region where evaporation takes place, the local heat transfer coefficient tends to be stable at about 70°. The local heat transfer coefficient decreases and film thickness increases at the bottom of the tube due to the accumulation of liquid film. Since regions of the upper apex and bottom account for a very small part of the circumferential length of the tube, both of the regions have little effect on the average heat transfer coefficients.

Contours of film temperature and vapor volume fraction as well as profiles of film thickness and average film velocity around two consecutive tubes are presented in Figs. 6–8. The given parameters for the three Figures are listed as inlet liquid temperature of 58°C, inlet spray density of 0.18 kg/m·s, tube wall temperature of 68°C, film evaporation temperature of 65°C, and tube pitch of 1.2. It can be seen in Fig. 8 that for the same circumferential position the film velocity outside the second tube is greater than that outside the first, and that the film thickness outside the second is thinner than that outside the first. This is due to the variety of liquid film physical property with liquid film temperature when liquid film flows from the first tube to the second one. Film velocities increase around the tube, then decrease at about 150°. Due to the accumulating and detaching effects of liquid film, film velocities decreases at the bottom of the tube. It is depicted in Figs. 6 and 7 that liquid film outside the second tube is all within the thermally developed region, and that the upper part of liquid film outside the first is within the thermally developing region. Therefore, a decreasing film viscosity in the second tube, caused by an increasing temperature, results in a decrease in flow resistance.

Fig. 9 shows profiles of heat transfer coefficients for pure water and seawater (salinity of 3.2%) at circumferential position of 45° as a function of Re and evaporation temperature. Heat transfer coefficients for pure water increase at a higher speed than those for seawater with an increase in evaporation temperature. A decrease in heat conduction and viscosity of liquid film with increasing evaporation temperature causes thinning film thickness and increasing film velocity, which results in enhancing the effect of conduction. A decrease in surface tension of pure water with an increase in evaporation temperature contributes to strengthening convective heat transfer. However, an increase in surface tension of seawater with evaporation temperature in the range of 62–82°C [24] dampens the convection heat transfer in liquid film. Although the conduction dominates in liquid film, the effect of the convective heat transfer can not be neglected due to the very thin film on the outside of the tube at the magnitude of mm.

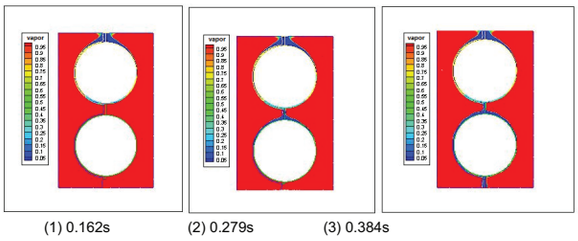

Fig. 6. Contours of vapor volume fraction: (a) 0.162 s, (b) 0.279 s, (c) 0.384 s.

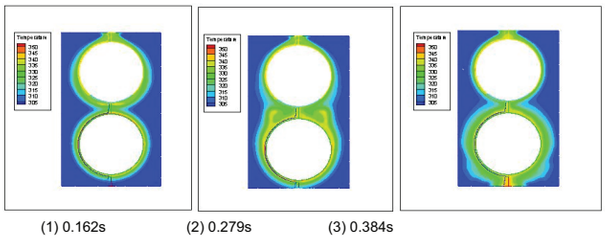

Fig. 7. Contours of temperature.

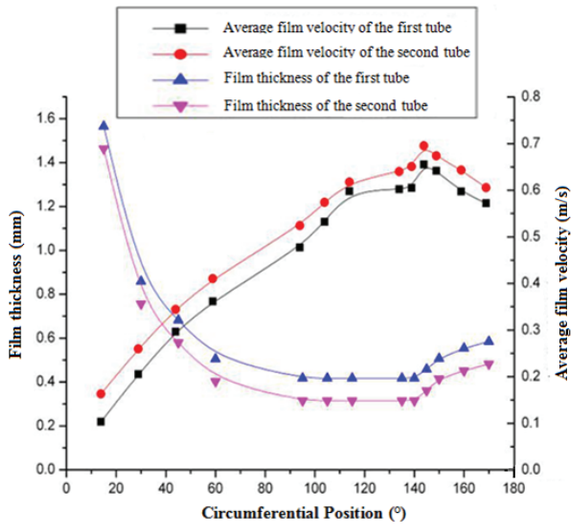

Fig. 8. Profiles of film thickness and average film velocity around two consecutive horizontal tubes: (a) sea water, (b) pure water.

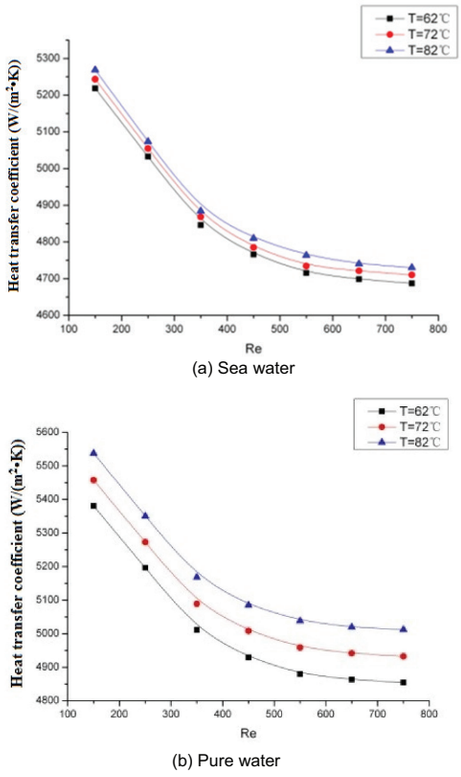

Fig. 9. Profiles of heat transfer coefficients for pure water and seawater at circumferential position of 45°.

4. Conclusions

A numerical model was developed to investigate the characteristics of hydrodynamics and heat transfer in falling film evaporation on a horizontal tube including local heat transfer coefficient, temperature, film thickness and velocity. A good agreement between simulation results and experimental data proves that the developed numerical model based on the VOF method is reliable and appropriate.

The variation of viscosity, surface tension and thermal conductivity in the liquid film has an obvious effect on the heat transfer coefficient even at low Reynold numbers. An increase in local heat transfer coefficient and a decrease in local film thickness along the tube circumference are observed in the thermal developing region due to the gravity effect and decreasing thermal conductivity. Local heat transfer coefficients stabilize at the bottom of the tube where the film is within the thermal developed region.

Acknowledgement

This work was supported by the National Natural Science Foundation of China (Grant No. 51576028).

Symbols

C_p	—	Specific heat, J/kg K
F	—	External body forces or momentum source, N/ m^3
g	—	Gravitational acceleration, m/s^2
h	—	Heat transfer coefficient, W/m^{2}K
h^+	—	Dimensionless heat transfer, coefficient
k	—	Thermal conductivity, W/m K
P	—	Pressure, Pa
Re	—	Reynold's number
S_m	—	Mass source, kg/m^{3}s
S_e	—	Energy source, W/m^3
t	—	Time, s
T	—	Temperature, °C or K
T_{sat}	—	Saturated temperature, °C or K
ΔT	—	Temperature difference between the wall and saturated temperatures, °C or K
u	—	Velocity in x-direction, m/s
v	—	Velocity in y-direction, m/s
$\vec{v}$	—	Velocity vector, m/s
x	—	Horizontal coordinate
y	—	Vertical coordinate
ρ	—	Density, kg/m^3
θ	—	Circumferential position, °
τ	—	Shear stress, N/m^2
Γ	—	Mass flow rate of liquid film per unit length, kg/m s
μ	—	Dynamic viscosity, Pa s

References

[1] L. Consolini, D. Robinson, J.R. Thome, Void fraction and two-phase pressure drops for evaporating flow over horizontal tube bundles, Heat Transfer Eng., 27 (2006) 1–18.
[2] R. Ulbrich, D. Mewes, Vertical, upward gas-liquid two-phase flow across a tube bundle, Int. J. Mult. Flow, 20 (1994) 249–272.
[3] G.R. Noghrehkar, M. Kawaji, A.M.C. Chan, Investigation of two-phase flow regimes in tube bundles under cross-flow condition, Int. J. Mult. Flow, 25 (1999) 857–874.
[4] B.L. Ruan, A.M. Jacobi, L.S. Li, Effects of a countercurrent gas flow on falling-film mode transitions between horizontal tubes, Exper. Thermal. Fluid Sci., 33 (2009) 1216–1225.
[5] X.f. Wang, A.M. Jacobi, A thermodynamic basis for predicting falling-film mode transitions, Int. J. Refriger., 43 (2014) 123–132.
[6] K. Ishiraha, J.W. Palen, J. Taborek, Critical review of correlations for predicting two-phase flow pressure drop across tube banks, Heat Transfer Eng., 1 (1980) 23–32.
[7] D.M. Robinson, J.R. Thome, Local bundle boiling heat transfer coefficients on an integral finned tube bundle, HVAC Res., 10 (2004) 331–344.
[8] D.M. Robinson, J.R. Thome, Local bundle boiling heat transfer coefficients on turbo-BII HP tube bundle, HVAC Res., 10 (2004) 441–458.
[9] R. Roser, B. Thonon, P. Mercier, Experimental investigations on boiling of n-pentane across a horizontal tube bundle: two-phase flow and heat transfer characteristics, Int. J. Refriger., 22 (1999) 536–547.
[10] R.A. Tatara, P. Payvar, Effects of oil on boiling of replacement refrigerants flowing normal to a tube bundle. Part II: R-134a, ASHRAE Trans., 106 (2000) 786–791.
[11] L. Aprin, P. Mercier, L. Tadrist, Analysis of Experimental Results of n-Pentane and Propane Boiling Across a Horizontal Tube Bundle, 12th International Heat Transfer Conf., Grenoble, France, 2002.
[12] R. Abraham, A. Mani, Effect of flame spray coating on falling film evaporation for multi-effect distillation system, Desal. Wat. Treat., 46 (2012) 1–8.
[13] A.T. Conlisk, The effect of coolant flow parameters on the performance of an absorber, ASHRAE Trans., 101 (1995) 73–80.
[14] A.T. Conlisk, A model for the prediction of the performance of a splined-tube absorber – Part 2: model and results, ASHRAE Trans., 102 (1996) 128–137.
[15] V.E. Nakoryakov, N.I. Grigor'eva, Analysis of exact solutions to heat- and mass-transfer problems for absorption with films or streams, Theor. Found. Chem. Eng., 31 (1997) 119–126.
[16] A. Ramadane, Z. Aoufoussi, H. Le Goff, Experimental investigation and modeling of gas-liquid absorption with a high thermal effect, distillation and absorption, Inst. Chem. Eng. Symp. Ser., 1 (1992) A451–A459.
[17] R. Abraham, A. Mani, L.S.S. Prakash Kumar, CFD studies on falling film modes in tube bundles in multi-effect distillation (MED) system, J. Environ. Sci., 1 (2013) 1–10.
[18] Q. Qiu, X. Zhu, L. Mu, S. Shen, Numerical study of falling film thickness over fully wetted horizontal round tube, Int. J. Heat Mass Transfer, 84 (2015) 893–897.
[19] L. Gong, S. Shen, H. Liu, X. Mu, X. Chen, Three-dimensional heat transfer coefficient distributions in a large horizontal-tube falling film evaporator, Desalination, 357 (2015) 104–116.
[20] R. Abraham, A. Mani, Heat transfer characteristics in tube bundles for falling film evaporation in multi-effect desalination system, Desalination, 51 (2013) 822–829.
[21] H. Raach, S. Somasundaram, J. Mitrovic, Optimisation of turbulence wire spacing in falling films performed with Open FOAM, Desalination, 267 (2011) 118–119.
[22] H. Raach, J. Mitrovic, Seawater falling film evaporation on vertical plates with turbulence wires, Desalination, 183 (2005) 307–316.
[23] H. Struve, Heat Transfer to an Evaporating Falling Refrigerant Film, The 12th Congress of the International Institute of Refrigeration, Madrid, 1967.
[24] P. Zhang, Study on the surface tension of sea water, J. Shanxi Normal Univ. Nat. Sci. Ed., 25 (2011) 44–45.
[25] M.H. Sharqawy, J.H. Lienhard, S.M. Zubair, Thermophysical properties of seawater: a review of existing correlations and data, Desal. Wat. Treat., 16 (2010) 354–380.